



ELSEVIER

Available online at [www.sciencedirect.com](http://www.sciencedirect.com)

 ScienceDirect

Ocean Engineering 33 (2006) 2209–2223

**OCEAN  
ENGINEERING**

[www.elsevier.com/locate/oceaneng](http://www.elsevier.com/locate/oceaneng)

Technical Note

# Pulsatile vortex generators for low-speed maneuvering of small underwater vehicles

Kamran Mohseni\*

*Department of Aerospace Engineering Sciences, University of Colorado, Boulder, CO 80309-0429, USA*

Received 20 June 2005; accepted 19 October 2005

Available online 27 March 2006

---

## Abstract

Compact zero-mass pulsatile jet actuators are proposed for low-speed maneuvering and station keeping of small underwater vehicles.<sup>1</sup> The flow field of such jets are initially dominated by vortex ring formation. Pinched-off vortices characterize the extremum impulse accumulated by the leading vortex ring in a vortex ring formation process. Relevant parameters in this process are identified in order to design simple and low cost zero-mass pulsatile jet actuators. Thrust optimization of synthetic jets for maximal thrust generation is achieved by enforcing the jet formation number to be around 4. Prototypes of such actuators are built and tested for underwater maneuvering and propulsion. The actuators could be used in two ways: (i) to improve the low-speed maneuvering and station keeping capabilities of traditional propeller driven underwater vehicles, and (ii) as a synthetic jet for flow control and drag reduction at higher cruising speeds. A model for calculating the rotation rate of the underwater vehicle is also proposed and verified.

© 2006 Elsevier Ltd. All rights reserved.

*Keywords:* Unmanned underwater vehicle; Pulsatile jets; Vortex ring; Pinch-off process; Maneuvering

---

---

\*Tel.: +1 303 492 0286; fax: +1 303 492 7881.

*E-mail address:* [mohseni@colorado.edu](mailto:mohseni@colorado.edu).

<sup>1</sup>Our research in this area was reported as the cover story of the *New Scientist* on October 23, 2004 (Frost Gorder, 2004, science writer).

## 1. Introduction

Oceans hold the key to the origin and continuity of life on the Earth. Three quarter of our planet's surface is covered by water where a richer biodiversity than life on land exists—more major taxonomic groupings of animals can be found in the oceans than on land. The oceans also form the largest reservoir on Earth for holding dissolved greenhouse gasses. Aside from providing food, energy, and mineral resources, oceans also play a critical role in regulating Earth's weather and climate, replenishing and maintaining the viability of our atmosphere, housing extraordinarily diverse forms of life, and significantly influencing the creation and ever-changing appearance of our coastlines. In summary, oceans affect the environment and life, as we know it, on a fundamental scale.

Although the oceans cover more than 70% of our planet's surface, much of the oceans have been investigated in only a cursory sense, and many areas have not been investigated at all. Some estimates suggest about 95% of the world's oceans and 99% of the ocean floor are unexplored ([Committee on Exploration of the Seas and the National Research Council, 2003](#)). Oceans are the last frontier on Earth—and the potential for discovery is largely untapped.

In the decades ahead, ocean scientists are poised to make major breakthroughs in understanding of ocean biology, chemistry, geology, and physics. Such potential has been created by an extraordinary period of invention and discovery from which new capabilities have emerged in the areas of computation, molecular biology, sensory and remote sensing technologies, underwater equipment and robotics, deep drilling, and rapid ocean-observing technologies. To this end, research and development on unmanned underwater vehicles (UUVs) have seen a significant surge over the last couple of decades due to mainly new materials, sensors, propulsion, navigational and guidance techniques, and theoretical and computational methods. UUVs are distinguished from conventional submarines by the absence of a crew. While applications of UUVs go back to self-propelled torpedoes designed in 1868 by Whitehead, the commercial potential of UUVs was not recognized up until the oil and gas discoveries in North Sea.

The term UUV is used here as a generic term describing both remotely operated vehicles (ROVs) and autonomous underwater vehicles (AUVs). To this end, a ROV is a marine craft operated by a human operator via a tethered cable or acoustic link, whilst an AUV is a marine vehicle operating without constant monitoring and supervision by a human operator. While ROVs are considered as the workhorses of the current offshore industry, AUVs represent the potential technology of future ocean exploration. AUVs are becoming increasingly important in the commercial realm because, unlike the ROVs, they do not require an escort ship or cable connection. Requiring only minor technical and logistic support, they can operate in regions into which no manned underwater vessel or ROV could penetrate (e.g., below the polar ice regions). However, many technical challenges such as navigation, guidance and control, endurance (battery power), and new propulsion and maneuvering technologies, as well as non-technical challenges such as legal liabilities and responsibilities for AUV deployments need to be resolved before such a dream is realized.

While there are many available UUV designs, most of them can be categorized in a few groups. Propeller thruster combined with control fins (or shrouded thrusters) to propel and steer the vehicle have traditionally been used in most AUV designs. These includes WHOI's REMUS, MIT's Odyssey, and Ocean Voyager II from Florida Atlantic University. Such designs are often streamlined (torpedo-like body shape) and optimized for low drag during forward motion. Maneuvering control forces are generated by lift or deflection forces created by fluid flow over the control surfaces. At cruising speeds, and for relatively uncluttered spaces, this paradigm is extremely efficient and effective. However, at low speeds and in tight spaces the magnitude of the available control forces drops significantly. Consequently, such vehicles are difficult to dock or operate at low speeds. As a result, much current effort is devoted to the development of docking mechanisms.

ROVs or AUVs, which are not designed for cruising, typically follow the so-called "box design". WHOI's ABE (Yoerger et al., 1998) and SeABED and Stanford's OTTER (Wang et al., 1995) are among AUVs in this category. Successful ROVs using box design include MBARI's Tiburon and WHOI's JASON (Yoerger et al., 1986). In box designs, better low-speed maneuvering (LSM) and control are achieved by sacrificing the low drag body-of-revolution design and adding multiple thrusters at different locations and directions. Propellers are very effective when they work at constant speed. However, they are less efficient for small motion corrections when the motions of propellers involve less than a full shaft rotation. This results in degraded control precision and possibly periodic oscillations of the vehicle's position. Continuous jet propulsion for underwater vehicles are reviewed in Allmendinger et al. (1990), Manen and Oossanen (1998). In particular, Downingtown–Huber-type pumps were recently proposed and their benefits were discussed for jet propulsion applications (Korde, 2004). Design and control issues of AUVs were reviewed by Yuh (2000) and for a review of guidance laws for UUVs the reader can consult Naeem et al. (2003) and the references therein.

In summary, underwater maneuvering (especially at low speeds) and docking procedures represent a major challenge in the design of AUVs and ROVs. To this end, this manuscript is focused on a novel LSM capability for underwater vehicles. We refer the reader to Webb (2004) and the references therein for other maneuvering techniques and issues associated with maneuverability. To this end, experimental platforms for testing, evaluating, and developing a LSM capability for UUVs are recently developed at the University of Colorado (see Baumann et al., 2003; Allgeier et al., 2004). A novel synthetic jet technology for operation in water is proposed here that could overcome many of the shortcomings described above for LSM of AUVs and ROVs, and enable new types of lower cost micro-AUVs (see Mohseni, 2004a,b and science writer). As described below, this propulsion scheme has no protruding components that increase drag, has very few moving parts, and takes up relatively little volume. Such hybrid designs which incorporate both a main propeller and a distributed set of pulsatile jets will improve low-speed AUV performance. While propellers clearly perform best at cruising speeds, pulsatile jets can significantly augment low-speed maneuverability, and enable occasional loitering/hovering actions. Such pulsatile jets can also implement drag-reducing flow control (similar

to what has been used in air by Glezer and Amitay (2002)) while the vehicle is cruising under propeller power.

This manuscript is organized as follows. Section 2 discusses the zero-mass pulsatile jet concept for propulsion and maneuvering. Our prototype synthetic jet actuator (SJA) is introduced in Section 3. Application of SJAs in UUVs is considered in Section 4, where a model for predicting the SJA thrust is also proposed and verified. Concluding remarks are presented in Section 5.

## 2. Zero-mass pulsatile jet propulsion

The propulsion scheme suggested here is loosely inspired by the propulsion of cephalopods (e.g. squid and octopi), salp, and jellyfish (Nixon and Messenger, 1977; O'Dor and Webber, 1986, 1991; Seikman, 1963; Trueman, 1968; Weihs, 1977). Squid (see Fig. 1) use a combination of fin undulations and a jet which can direct thrust at any angle through a hemisphere below the body plane. Their complete range of locomotory behavior rivals that of reef fish. Jet propulsion swimming of the squid is accomplished by drawing water into the mantle cavity, and then contracting the mantle muscles to force water out through the funnel. The funnel, which is directly behind and slightly below the head, can be maneuvered so as to direct jets in a wide range of directions. Another example of pulsatile jet locomotion is jellyfish swimming (DeMont and Gosline, 1988), which relies upon repeated contractions of an umbrella-shaped structure, or bell. During contraction, circular subumbrellar muscles pull the sides of the bell inward, reducing the volume of the subumbrellar cavity, and forcing water out through the velar aperture. Water is drawn back into the subumbrellar cavity during the relaxation phase. The jellyfish can optimize its propulsion by controlling the diameter, velocity, and profile at the exit of the velar aperture.

Starting jets are usually characterized by the roll up of the ejected shear layer from a nozzle or an orifice and the formation of vortex rings; see Fig. 2. Vortex rings has captured the attention of many researchers over the last century. Vortex rings have

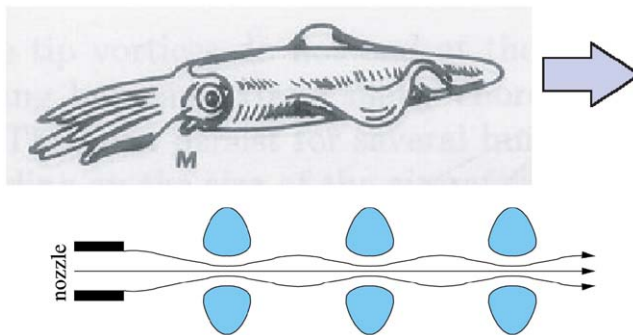


Fig. 1. Squid locomotion by pulsed jet.

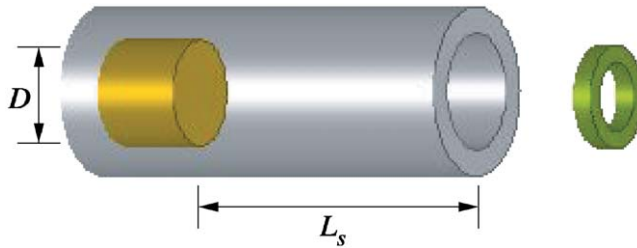


Fig. 2. Cylinder piston mechanism.

relatively simple and persistent three-dimensional structure and at high Reynolds numbers they decay slowly. The generation, formation, evolution, and interactions of vortex rings have been the subject of numerous investigations (see, e.g. Shariff and Leonard, 1992 and the references therein). In this study, we focus our attention on a specific characteristic of vortex ring formation; namely the impulse extremization in vortex ring formation and its connection with the vortex ring pinch-off phenomenon.

Weihs (1977), Seikman (1963), and recently Krueger and Gharib (2003, 2005) and Mohseni (2002) have shown that a pulsed jet can give rise to a greater average thrust force than a steady jet of equivalent mass flow rate. In a pulsed jet, an ejected mass of fluid rolls into a toroidal vortex ring which moves away from its source. A continuously pulsatile jet, therefore, produces a row of vortex rings (see Fig. 1). At high pulsing frequency, the jet structure can become increasingly turbulent.

Vortex ring jets can be generated using a variety of mechanical devices. While a squid generates vortex rings by muscle contraction around the mantle, one of the simplest ways to generate vortex rings and pulsatile jets in the laboratory is the motion of a piston pushing a column of fluid through an orifice; the so-called cylinder–piston mechanism (see Fig. 2). This system provides a simplified approximation to natural pulsatile jet generation, and it is amenable to experimental, computational, and analytic study. When the piston pushes fluid through the cylinder, the boundary layer of the fluid expelled from the cylinder will separate and roll up into a vortex ring at the orifice edge. Experiments by Gharib et al. (1998) have shown that for large enough ratios of piston stroke versus diameter ( $L/D$ ), the generated flow consists of a leading vortex ring followed by a trailing jet. See Fig. 3(a) for experimental results, and Fig. 3(b) for corresponding numerical simulations.

It was both experimentally Gharib et al. (1998) and analytically Mohseni and Gharib (1998) observed that the limiting stroke  $L/D$  occurs when the generating apparatus is no longer able to deliver energy, circulation and impulse at a rate comparable with the requirement that a steadily translating vortex ring has maximum energy with respect to kinematically allowable perturbations. Mohseni and Gharib (1998) suggest that the properties of the leading vortex ring are the final outcome of a relaxation process, dependent only on the first few integrals of the motion (the energy,  $E$ , impulse,  $I$ , and circulation,  $\Gamma$ ). Mohseni (2001a) argued that the energy extremization in Kelvin's variational principle has a close connection with the entropy maximization in statistical equilibrium theories. Numerical evidence for

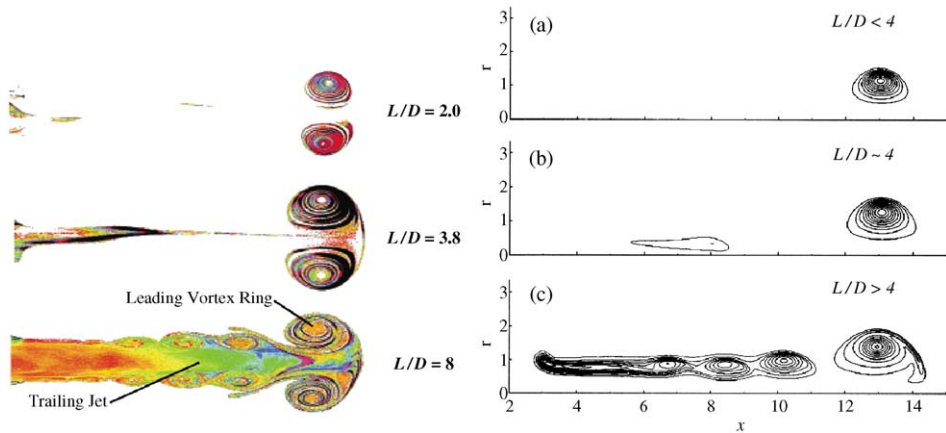


Fig. 3. (Left) Experimentally obtained fluid vorticity profiles during the vortex ring pinch-off process (for various  $L/D$  formation numbers) from Gharib et al. (1998). (Right) Numerical simulation of vortex ring formation at various formation numbers, from Mohseni et al. (2001). Only one-half of the symmetric jet cross section is presented.

a relaxation process in axisymmetric flows to an equilibrium state has been provided by Mohseni et al. (2001) in a direct numerical simulation of the vortex ring pinch-off process. Similar phenomena are observed in the alternating vortex shedding behind bluff bodies (Mohseni, 2001b).

In squid and jellyfish, the exit diameter of the cylinder (mantle or bell) varies during the expulsion of fluid. This technique optimizes propulsive output. We have recently shown that a time varying shear layer velocity mechanism can also manipulate pulsatile jet behavior (see Mohseni and Gharib, 1998; Mohseni et al., 2001). While the mechanisms here are even more complicated than the piston–cylinder model, this model does provide useful guidance on the overall physical phenomena at work.

### 3. Synthetic jet actuator (SJA) prototypes

While the piston–cylinder model is attractive for theoretical studies and ease of experimental setup, there are more practical means to generate pulsatile jets. To this end, prototypes of pulsatile jet generators using the Helmholtz cavity concept are designed and built in this investigation. Various actuation techniques can be employed for actuating the diaphragm. These includes, but not limited to, using solenoid plungers, acoustic speakers, electrostatic, and piezoelectric actuation. In this design, the inward movement of a diaphragm draws fluid into a chamber (Fig. 4). The subsequent outward diaphragm movement expels the fluid, forming a vortex ring or a jet depending on the formation number. Repetition of this cycle results in a pulsatile jet. Because of the asymmetry of the flow during the inflow and

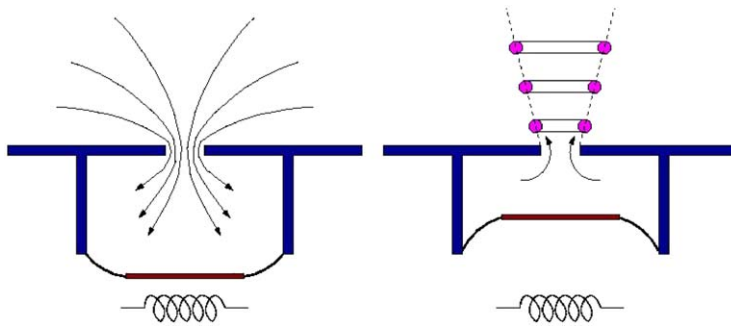


Fig. 4. Synthetic jet actuator concept: (Top) Fluid entrainment; (Bottom) vortex ring formation.

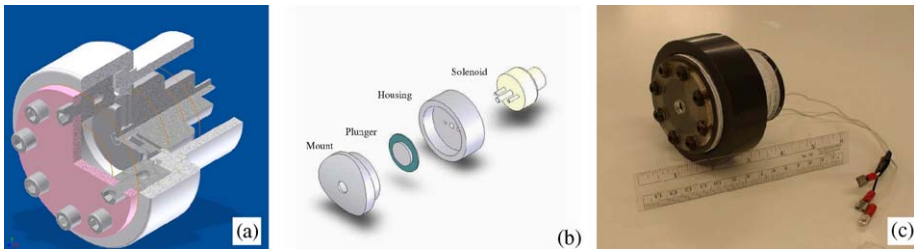


Fig. 5. CU boulder synthetic jet prototype: (a) CAD model of the actuator design. (b) Plunger and solenoid assembly. (c) Actual fabrication of the synthetic jet actuator.

outflow phases, a net fluid impulse is generated in each cycle, even though there is no net mass flow through the chamber over one cycle.

Fig. 5 shows the structure and appearance of a pulsatile jet actuator prototype (see also Mohseni, 2004a,b). The driving diaphragms consist of a rigid disk with a flexible surround. Currently, a solenoid actuator is used to generate the diaphragm motion. A voice coil driven synthetic jet prototype is reported in Polsenberg-Thomas et al., (2005). The fluid pushed by the moving diaphragm exits through an orifice. The experimental prototypes also allows easy substitution of different sized orifices and different sized chambers. In this way, physical parameters can be easily varied so that theoretical models (see below) can be compared against actual experimental results in different parameter regimes. This design has many advantages including its simplicity, very few moving parts, compactness, and no high tolerance (and therefore costly) components.

In order to quantify thrust generation, we have designed and build a new synthetic jet actuator that will give us the ability to change many design parameters. These includes, actuation frequency and amplitude, diaphragm velocity profile, cavity geometry (height, diameter, and exit geometry), nozzle height and diameter, etc. The new prototype is shown in Fig. 6. In the current design, the motion of the diaphragm, the frequency and amplitude of actuations, the exit diameter and

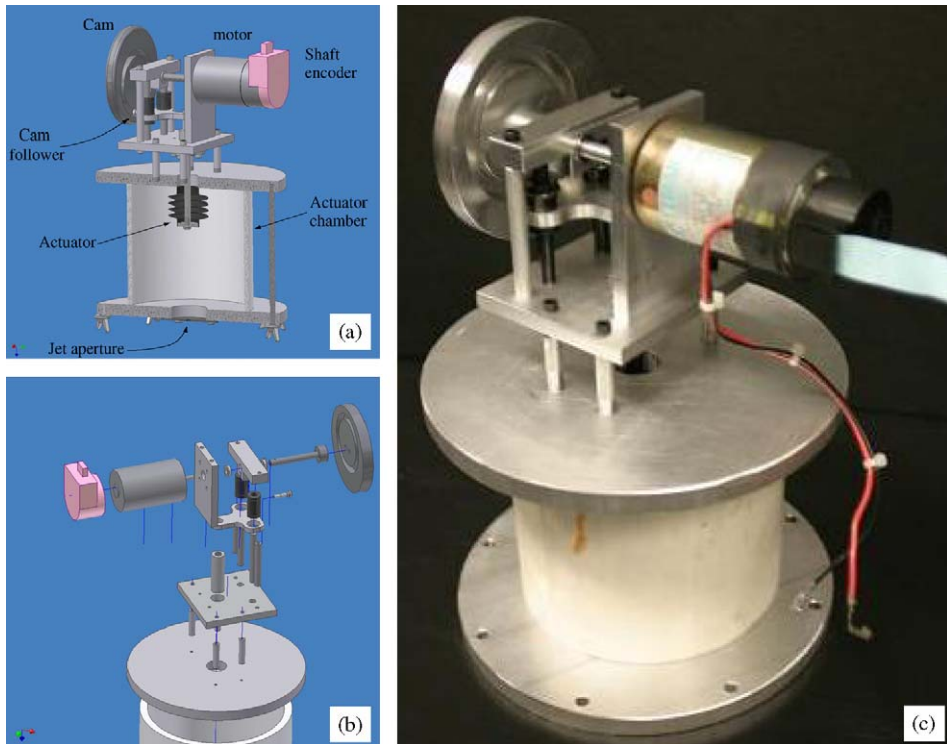


Fig. 6. Second generation of synthetic jet prototypes capable of changing many actuation parameters: (a) CAD model of the actuator design. (b) Actuator assembly. (c) Actual fabrication of the synthetic jet actuator.

the height and diameter of the cavity can be easily controlled. A cam mechanism is used to convert rotary motion into pre-defined reciprocating motion.

#### 4. Pulsatile jet UUV prototype

Special design of UUVs are required in order to implement, demonstrate, and evaluate fully maneuverable self-contained hybrid underwater vehicles that combines pulsatile jet actuators with propeller-based propulsion schemes. To this end, the first phase of designing, building, and testing a remote controlled (RC) underwater vehicle was completed at the University of Colorado. While RC application in water is not practical for field tests, it was suitable for test in controlled environment in a pool in this investigation. Another option was tethered vehicle. The first version of the our vehicle is 1.4 m long, uses a conventional propeller and control surfaces, and is remotely controlled up to 5 ft depth. Below this depth, communication with the vehicle is not reliable. The vehicle is designed with 1% positive buoyancy, so in case of communication loss, the vehicle comes up to the surface.

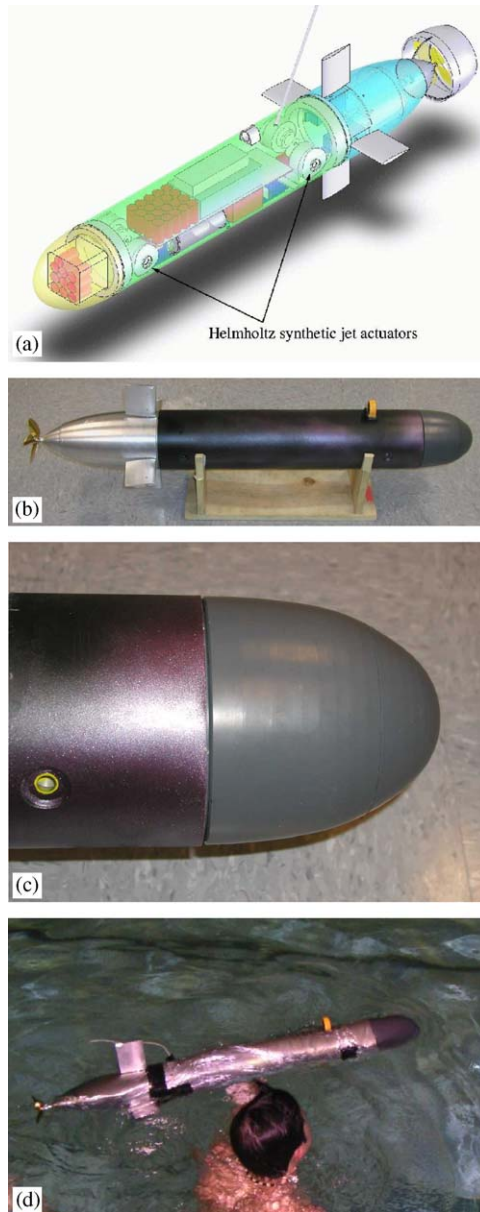


Fig. 7. UUV test-bed at the University of Colorado. (a) CAD model of the Colorado UUV with SJAs. (b) Colorado UUV. (c) Exit nozzle of the SJA on the Colorado UUV. (d) Test of the Colorado UUV in the pool.

A new lighter and shorter (around 1 m) underwater vehicle was also designed and built. The new vehicle, remote aquatic vehicle (RAV), can house up to four SJAs within the vehicle body, and have an active buoyancy system (see Fig. 7). RAV will

be used as a platform for testing the performance of the SJAs for low-speed turning capabilities and high-speed drag reduction. RAV is also designed with an expandable payload section capable of carrying various sensors for telemetry. This vehicle will serve as a model test-bed for hybrid vehicle designs that combine pulsatile jets with conventional propellers and torpedo-like bodies.

The input design parameter for LSM of UUVs is the revolution per minute (RPM) turn rate requirement or equivalently the angular velocity  $\omega$ . From the required RPM one can calculate the drag moment experienced by the vehicle. We estimate the drag forces experienced by a submerged tube (see Fig. 8) in rotation around an axis normal to its symmetry line. Since a differential element of the tube at a radial distance of  $r$  away from the rotation axis has a local velocity of  $V = r\omega$ , which increases with distance from the rotation axis, the differential elements experience different drag forces. These forces can be estimated from drag data for flow behind a cylinder with diameter  $d$  at the local Reynolds number  $Re = (r\omega)d/v$ . Note that three-dimensional, cross-flow, and flow-vehicle interaction effects are ignored in this simplified analysis. The total drag moment of a tube of length  $L$  rotating with an angular velocity of  $\omega$  around its middle can be approximated by (ignoring external flow effects)

$$M_{\text{drag}} = 2 \int_0^{L/2} \frac{1}{2} r d \rho (r\omega)^2 C_D dr$$

or by changing the integration variable to the local Reynolds number  $Re$

$$M_{\text{drag}} = \rho \frac{v^4}{\omega^2 d^3} \int_0^{Re_{L/2}} Re^3 C_D(Re) dRe, \quad (1)$$

where  $C_D$  is the drag coefficient behind a cylinder at the local Reynolds number. The SJAs are expected to provide at least equal moment on the vehicle to overcome the drag moment.

In order to estimate the moment produced by the SJAs, a *slug model* (see e.g. Mohseni and Gharib, 1998; Dabiri and Gharib, 2004) is used to approximate the thrust or impulse during the jet expulsion from the Helmholtz cavity. We approximate the initial state by a column of fluid with diameter  $D = 2R$  and length  $L_s$  moving at a constant velocity  $U_j$  (average jet velocity). The slug model is

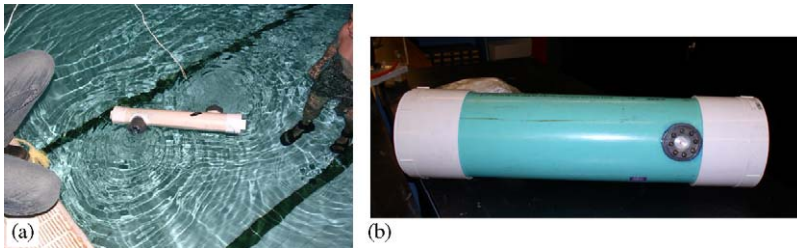


Fig. 8. Test of the synthetic jet actuator. (a) Using SJAs to rotate a 4.5 in diameter tube. (b) Installation of SJAs on an 8 in diameter tube, illustrating minimal impact of actuator on hull design.

characterized by the following relations for the energy  $E$ , circulation  $\Gamma$ , and impulse  $I$  of the ejected fluid:

$$E = \frac{1}{8} \pi D^2 L_s U_j^2 = \frac{I\Gamma}{L_s}, \tag{2}$$

$$\Gamma = \frac{L_s U_j}{2} = \frac{I}{2\pi R^2}, \tag{3}$$

$$I = \frac{1}{4} \pi D^2 L_s U_j = \frac{1}{2} \pi D^2 \Gamma. \tag{4}$$

The slug model provides an estimate of the invariants of motion initially injected in the medium. We assume the optimal formation number of  $L_s/D \approx 4$  (Gharib et al., 1998; Mohseni and Gharib, 1998; Mohseni et al., 2001; Mohseni, 2001a) for the ejecting slug of fluid with length  $L_s$  and the jet exit diameter  $D$ . Since water is incompressible, the volume of the ejected jet (see Fig. 9)

$$V_s = \frac{\pi D^2}{4} L_s$$

is equal to the volume displacement of the Helmholtz cavity due to the displacement of the diaphragm; in this case

$$V_D = \frac{\pi h}{8} (D_{ca}^2 + D_{cy}^2),$$

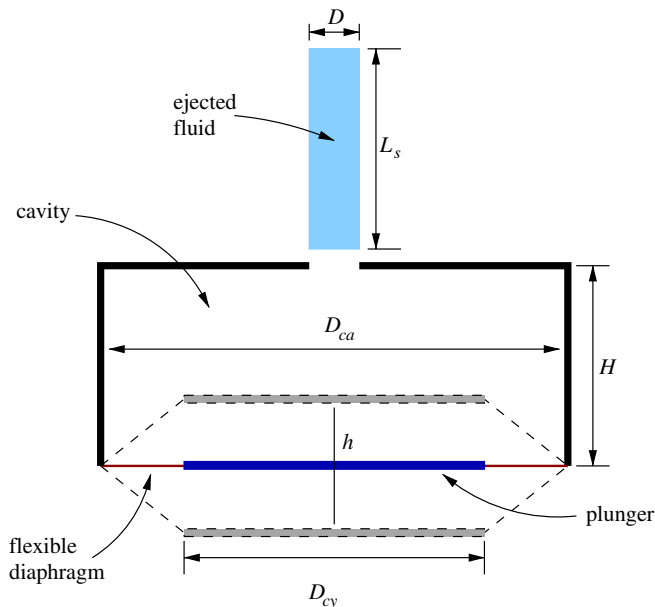


Fig. 9. Actuation of a synthetic jet actuator.

where  $h$  is the plunger stroke and  $D_{ca}$  and  $D_{cy}$  are the diameter of the cavity and the plunger, respectively. Consequently, the exit diameter (assuming  $L_s/D \approx 4$ ) is related to the stroke length of the plunger (or diaphragm) through

$$\frac{L_s}{h} = \frac{D_{ca}^2 + D_{cy}^2}{2D^2}.$$

Therefore, for optimal vortex formation, assuming  $L_s/D \approx 4$

$$D^3 = \frac{h}{8}(D_{ca}^2 + D_{cy}^2) \quad \text{or} \quad L_s^3 = 8h(D_{ca}^2 + D_{cy}^2).$$

By knowing the stroke length of the plunger and its frequency one can easily estimate the generated impulse from the slug model to be  $\rho\pi D^2 L_s U_j/4$ , where  $\rho$  is the fluid density and  $U_j = 2L_s f$  is the exiting jet velocity (proportional to the plunger velocity) during the expulsion period. An estimate of the moment produced by the SJAs can now be easily obtained by multiplying the SJA force with its moment arm. For a pair of actuators with a separation distance of  $l$  the net moment  $M_{SJA}$  can be estimated to be

$$M_{SJA} = 16\pi\rho D^4 f^2 l. \tag{5}$$

Results of these calculation for the 4.5 in test tube shown in Fig. 8(a) are reported in Fig. 10. In order to accommodate for the reverse momentum during the ingestion

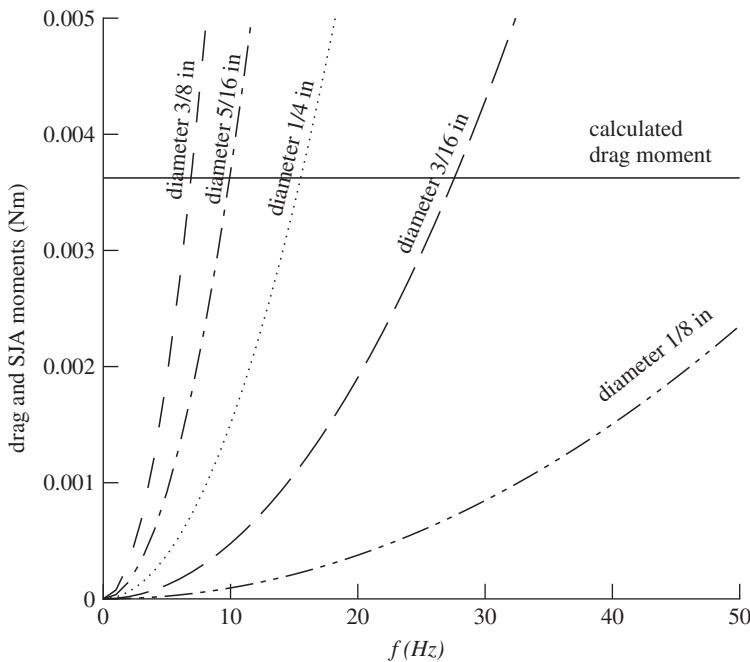


Fig. 10. Thrusting moment versus actuation frequency for various exit diameter at one rpm.

part of the actuation a momentum adjustment factor of two is used. This is justified based on the calculations reported by Mittal et al. (2001) for micro-synthetic jets in air environment. Calculated momentum drag in Eq. (1) is also shown in the figure. The part of the SJA moment curves above the drag moment value represents enough actuation moment to overcome the drag. Fig. 10 shows that the required drag moment can be overcome with various actuator exit diameters consistent with the optimal formation number of 4. Therefore, for a given solenoid stroke, one can estimate the optimal length of the ejected fluid, exit diameter, and attainable rotation rate of the submerged tube. Similarly, the velocity of the solenoid actuation (or its frequency) can be related to the jet velocity at the exit of the cavity. Consequently, for a given cavity geometry, exit diameter, solenoid actuation frequency, and solenoid stroke, one can calculate the SJA moment. This is also depicted in Fig. 10 as a function of the actuation frequency for various exit diameters.

Larger exit diameters require less actuation frequency, and higher solenoid force for the specified duty cycle. The ability of the SJAs to rotate a submerged tube was demonstrated as depicted in Fig. 8 in order to validate the models presented in this section. Our test results closely matched the hydrodynamic thrust model of Fig. 10. More detailed account of the effect of various actuation parameters ( $D$ ,  $D_{ca}$ ,  $D_{cy}$ ,  $f$ , velocity profile of the diaphragm, exit hole length, cavity and exit hole geometry) is the subject of a future publication.

## 5. Conclusions

A novel mechanism for LSM of underwater vehicles is proposed, where compact zero-net mass pulsatile jet actuators are employed to achieve maneuvering capability at low speeds without sacrificing the low drag body-of-revolution designs. The same actuation mechanism could be potentially used as a flow control and drag reduction device at higher cruising speeds, when a propeller is employed for propulsion. The actuation mechanism is simple, has very few moving parts, has no protruding components that increase drag, and takes up relatively little volume. It is expected that such a hybrid design which incorporate both a main propeller and a distributed set of pulsatile jets to improve low-speed UUV performance.

The synthetic jet actuators are designed based on the required moment to overcome the drag moment of the underwater vehicle at a given rotation rate. Simple equations are derived in order to calculate the vehicle's drag moment and the generated moment of the actuators. Consequently, by knowing the geometrical characteristics of the underwater vehicle and its required rotation rate one can design a zero-mass pulsatile jet actuators to accommodate the rotation requirement. The most relevant parameters in the design of the actuators are the plunger stroke and diameter, cavity diameter, jet exit diameter, and actuation frequency. While such zero-mass pulsatile jets can be used for maneuvering of underwater vehicles at low speeds, the same mechanism could be used as a synthetic jet for high-speed flow control around the vehicle and drag reduction.

## Acknowledgement

The research in this paper was partially supported by the National Science Foundation contract 0413300. The underwater vehicles in Fig. 7 were designed as part of senior projects supervised by K. Mohseni and S. Palo in academic years 2002–2003 and 2003–2004. The author would like to acknowledge the help from the involved students: M. Baumann, W. Dalbec, E. DeKruif, I. Morikawa, J. Novick, and M. Schade for the HydroBuff UUV and M. Allgeier, K. DiFalco, D. Hunt, D. Maestas, S. Nauman, J. Poon, and A. Shileikis for the RAV. The actuator in Fig. 5(c) was designed as part of a summer independent study under the supervision of K. Mohseni by L. Copperberg, L. Georgieva, C. Madsen, L. McCrann, and E. Thomas. The author would like to thank S. Palo and M. Rhodes for his contribution to the development of Colorado UUVs. The author also benefited from discussions with J.E. Marsden and J. Burdick on control aspects of UUVs.

## References

- Allgeier, M., DiFalco, K., Hunt, D., Maestas, D., Nauman, S., Poon, J., supervised by Mohseni, K., Shileikis, A., Palo, S., 2004. Senior design project: Remote Aquatic Vehicle, April 2004.
- Allmendinger, E.E., DeLavergne, M., Jackson, H., 1990. Hydrodynamical principles. In: Allmendinger, E.E. (Ed.), *Submersible Vehicle Systems*. Society of Naval Architects and Marine Engineers, New Jersey, USA, pp. 191–261.
- Baumann, M., Dalbec, W., DeKruif, E., Morikawa, I., Novick, J., Rhodes, M., supervised by Mohseni, K., Schade, M., Palo, S., 2003. Senior design project: Hydrobuff R5L unmanned underwater vehicle, April 2003.
- Committee on Exploration of the Seas and the National Research Council, 2003. *Exploration of the Seas: Voyage into the Unknown*, fifth ed. National Academic Press, Washington, DC.
- Dabiri, J.O., Gharib, M., 2004. A revised slug model boundary layer correction for starting jet vorticity flux. *Theoretical and Computational Fluid Dynamics* 17 (4), 293–295.
- DeMont, E., Gosline, J., 1988. Mechanics of jet propulsion in the hydromedusan jellyfish, *polyorchis penicillatus*. *Journal of Experimental Biology* 134, 347–361.
- Frost Gorder, P. (science writer), 2004. Search for the perfect vortex: vortex drive. *New Scientist* 184 (2470), 30–34.
- Gharib, M., Rambod, E., Shariff, K., 1998. A universal time scale for vortex ring formation. *Journal of Fluid Mechanics* 360, 121–140.
- Glezer, A., Amitay, M., 2002. Synthetic jets. *Annual Review of Fluid Mechanics* 34, 503–529.
- Korde, U.A., 2004. Study of a jet-propulsion method for an underwater vehicle. *Ocean Engineering* 31, 1205–1218.
- Krueger, P.S., Gharib, M., 2003. The significance of vortex ring formation to the impulse and thrust of a starting jet. *Physics Fluids* 15 (5), 1271–1281.
- Krueger, P.S., Gharib, M., 2005. Thrust augmentation and vortex ring evolution in a fully pulsed jet. *AIAA Journal* 43 (4), 792–801.
- Van Manen, J.D., Van Oossanen, P., 1998. Other propulsion devices. In: Lewis, E.V. (Ed.), *Principles of Naval Architecture*. Society of Naval Architects and Marine Engineers, New Jersey, USA, pp. 225–240 [Chapter 6, Section 10].
- Mittal, R., Rampungoon, P., Udaykumar, H.S., 2001. Interaction of a synthetic jet with a flat plate boundary layer. *AIAA paper* 2001-2773.
- Mohseni, K., 2001a. Statistical equilibrium theory of axisymmetric flows: Kelvin's variational principle and an explanation for the vortex ring pinch-off process. *Physics Fluids* 13 (7), 1924–1931.

- Mohseni, K., 2001b. Studies of two-dimensional vortex streets. AIAA paper 2001-2842. June 2001b. 31st AIAA Fluid Dynamics Conference and Exhibit, Anaheim, CA.
- Mohseni, K., 2002. Mixing and impulse extremization in microscale vortex formation. In: Proceedings of the Fifth International Conference on Modeling and Simulation of Microsystems, San Juan, Puerto Rico, April 2002.
- Mohseni, K., 2004a. Impulse extremization in synthetic jet actuators for underwater locomotion and maneuvering. In: Proceedings of the 23rd International Conference on Offshore Mechanics and Arctic Engineering. Vancouver, Canada, 20–25 June 2004a. Also published as a chapter in: Chwang, A.T., Teng, M.H., Valentine, D.T. (Eds.), *Advances in Engineering Mechanics, Reflections and Outlooks: In Honor of Theodore Y.-T. Wu*, World Scientific Publishing Company, Singapore, 2005.
- Mohseni, K., 2004b. Pulsatile jets for unmanned underwater maneuvering. AIAA paper 2004-6386, Chicago, IL, 20–23 September 2004b. Third AIAA Unmanned Unlimited Technical Conference, Workshop and Exhibit.
- Mohseni, K., Gharib, M., 1998. A model for universal time scale of vortex ring formation. *Physics Fluids* 10 (10), 2436–2438.
- Mohseni, K., Ran, H., Colonius, T., 2001. Numerical experiments on vortex ring formation. *Journal of Fluid Mechanics* 430, 267–282.
- Naeem, W., Sutton, R., Ahmad, S.M., Burns, R.S., 2003. A review of guidance laws applicable to unmanned underwater vehicles. *Journal of Navigation* 56, 15–29.
- Nixon, M., Messenger, J.B. (Eds.), 1977. *The Biology of Cephalopods*. Academic Press, London.
- O'Dor, R.K., Webber, D.M., 1986. The constraints on cephalopods: why squid aren't fish. *Canadian Journal of Zoology* 64, 1591–1605.
- O'Dor, R.K., Webber, D.M., 1991. Invertebrate athletes: trade-offs between transport efficiency and power density in cephalopod evolution. *Journal of Experimental Biology* 160, 93–112.
- Polsenberg-Thomas, A.M., Dabiri, J., Mohseni, K., Burdick, J., 2005. An experimental investigation and modeling of voice-coil driven synthetic jet propulsors for underwater vehicles. In: Proceedings of the International Symposium on Unmanned Untethered Submersible Technology, Durham, New Hampshire, August 21–24.
- Seikman, J., 1963. On a pulsating jet from the end of a tube, with application to the propulsion of aquatic animals. *Journal of Fluid Mechanics* 15, 399–418.
- Shariff, K., Leonard, A., 1992. Vortex rings. *Annual Review of Fluid Mechanics* 34, 235–279.
- Trueman, E.R., 1968. Motor performance of some cephalopods. *Journal of Experimental Biology* 49, 495–505.
- Wang, H.H., Marks, R.L., McLain, T.W., Fleischer, S.D., Miles, D.W., Sapilewski, G.A., Rock, S.M., 1995. Otter: a testbed submersible for robotics research. In: ANS 1995.
- Webb, P.W., 2004. Maneuverability—general issues. *IEEE Journal of Oceanic Engineering* 29 (3), 547–555.
- Weihs, D., 1977. Periodic jet propulsion of aquatic creatures. In: Nachtigal, W. (Ed.), *Bewegung-sphysiologie—Biomechanik*, pp. 171–175.
- Yoerger, D., Newman, J., Slotine, J.-J., 1986. Supervisory control system for the Jason ROV. *IEEE Journal of Oceanic Engineering* 11 (3), 392–400.
- Yoerger, D.R., Bradley, A.M., Walden, B.B., et al., 1998. Surveying a subsea lava flow using the autonomous benthic explorer (abe). *International Journal of Systems Science* 29 (10), 1031–1044.
- Yuh, J., 2000. Design and control of autonomous underwater robots: a survey. *Autonomous Robots* 8, 7–24.